


Paper Type: Original Article

## Experimental Investigation of Skin-Friction Drag Reduction over a Flat Plate Using Rectangular Obstacles in a Turbulent Boundary Layer

Rita De Fátima Muniz<sup>1,\*</sup> , Soheyla Sojodi<sup>2</sup>

<sup>1</sup> Postgraduate Program in Education, Center for Educational Assessment, Federal University of Ceará, 60430-160 Fortaleza, Brazil; ritafatimamuniz@gmail.com.

<sup>2</sup> Department of Mechanical Engineering, University of Guilan, Rasht, Iran; soheila\_sojodi@yahoo.com.

Citation:

Received: 12 April 2023  
Revised: 27 June 2023  
Accepted: 14 August 2023

Muniz, R. D. F., & Sojodi, S. (2024). Experimental investigation of skin-friction drag reduction over a flat plate using rectangular obstacles in a turbulent boundary layer. *Mechanical Technology and Engineering Insights*, 1(3), 152-159.


### Abstract


The current study aimed to evaluate the influence of rectangular obstacles with different aspect ratios on the skin friction coefficient of a flat plate in a turbulent boundary layer, using experiments in a suction-type wind tunnel with the floating-element technique. Obstacles having rectangular shapes with various  $c/t$  ratios of 2, 4, 8, and 18 were placed within the turbulent boundary layer at a distance of 2 mm from the flat plate surface. Four distinct values of Reynolds numbers at various free-stream velocities of 10, 11, 12, and 14 m/s were used for testing purposes. First, the experimental system was verified by comparing the skin-friction coefficients for a smooth flat plate with those obtained from an analytical correlation of the turbulent boundary-layer flow. The validation study results indicated excellent agreement between the experimental data and the analytical solutions. It was observed that mounting rectangular obstacles had a substantial effect on reducing the skin friction coefficient compared to the case without obstacles. The smallest value of the skin-friction coefficient was obtained for the obstacle with an aspect ratio  $c/t = 2$ . Moreover, as the Reynolds number increased, the skin friction coefficient decreased. The results above confirm that the mutual interaction between the generated vortices and the turbulent boundary layer modifies the flow characteristics, resulting in lower wall shear stress. This study shows that appropriately shaped rectangular obstacles can reduce turbulent skin friction drag, which may help reduce drag.

**Keywords:** Skin-friction drag reduction, Turbulent boundary layer, Rectangular obstacles, Aspect ratio, Floating-element technique.

## 1 | Introduction

The drag force, which is caused by the friction between the surface of the body and the fluid, is one of the most difficult forces to maintain motion. Examples of drag forces include the wings of an airplane, heat

 Corresponding Author: ritafatimamuniz@gmail.com

 <https://doi.org/10.48313/mtei.v1i3.58>



Licensee System Analytics. This article is an open access article distributed under the terms and conditions of the Creative Commons Attribution (CC BY) license (<http://creativecommons.org/licenses/by/4.0>).

exchangers, and turbine blades. Recently, attempts have been made to counteract these forces through flow control. One such way in which this objective is achieved is by placing rectangular obstacles in the flow field in proximity to the surface of the body. Because of stagnation points, jets between the obstacle and the plate, and the formation of vortices, the presence of these obstacles greatly affects the surface friction coefficient. This, however, depends on both the aspect ratio ( $c/t$ ) and the distance of the obstacle from the plate. Investigations in this area have mostly used numerical methods.

Parker and Welsh [1] were followed by Stokes and Welsh [2], who proposed four vortex-shedding patterns depending on the aspect ratio ( $c/t$ ). If  $c/t < 3.2$ , the detached shear layer will directly affect the trailing edge to form Kármán vortices. If  $3.2 < c/t < 7.6$ , the detached shear layer will keep separating and reattaching itself to form a new vortex region.

Finally, when  $7.6 < c/t < 16$ , the shear layer remains attached at all times to form scattered vortices. Lastly, for  $c/t > 16$ , the shed vortices affect the upstream region of the trailing edge, causing the detachment of the boundary layer, and subsequently Kármán vortex formation.

Nakamura and Nakashima [3], in their experimental work, termed the shear layer in the second case an "impinging shear layer" with a constant frequency. Naudascher and Wang [4] defined the first and second cases, respectively, as leading-edge vortex shedding and trailing-edge vortex shedding flows.

Park [5] conducted a numerical study on the effect of the distance between a square cylinder and the channel wall in unsteady flow at Reynolds numbers 50 and 150 with gaps from 0.1 to 1. The results showed that reducing the gap reduced the Strouhal number and stabilized the flow.

The effect of spacing variation between an 8 mm-diameter cylinder and a flat plate on the friction coefficient of the plate was studied by Marumo et al. [6], who found a reduction in friction at a spacing of 4 mm. It has been experimentally demonstrated by Suzuki and Suzuki [7] that the spacing between the cylinder and flat plate affects friction reduction more than the cylinder diameter.

The effect of a reduction in the friction coefficient and the generation of a clockwise vortex creating the reverse flow in the interaction of a turbulent boundary layer with the wake flow created behind the cylinder was confirmed by De Souza et al. [8] experimentally. A multi-objective optimization of the size and spacing of a trapezoidal shape object was done by Kahrom et al. [9] using a genetic algorithm for obtaining the optimum design of minimum friction coefficient and minimum frontal area of the flow. Over the past few years, several experimental and numerical investigations have examined the influence of obstacles on turbulent boundary layers and on skin friction reduction. The effect of boundary layer thickness on vortex shedding around a rectangular cylinder mounted on a wall has been experimentally studied by El Hassan et al. , who found that the interaction between the horseshoe vortex system and the large-scale wake is highly influenced by boundary layer thickness.

Isaev et al. [11] investigated the effect of the gap geometry between a rib and a flat plate on the near-wall flow structure and found that the gap geometry influences the near-wall flow structure. Inspired by biological designs, Domel et al. [12] have developed shark-skin-inspired designs to improve aerodynamic performance. At this point, the separation bubbles that develop around riblet formations impact the pressure distribution in such a way as to produce longitudinal vortices that counteract the reduction of momentum due to the presence of friction.

Yang et al. [13] observed, using TR-PIV methods, that riblets reduce drag by about 11%. In their work on drag reduction via the suppression of large coherent structures in turbulent Couette flows, Andreolli et al. [14] reported that the removal of these structures was directly related to reduced drag.

The effect of transverse rectangular gaps on boundary layer transition has been analyzed by Beguet et al. [15]. The authors developed a  $\Delta N$ -based scheme to predict the onset of flow instability caused by transverse gaps in boundary layers. In a study aimed at analyzing the effects of the aspect ratio ( $AR = 0.25-4$ ) and Reynolds number ( $Re = 100-180$ ) on the flow past three side-by-side rectangular cylinders, Rahman et al. [16] used

lattice Boltzmann simulations. They observed that AR had a stronger effect than Re. The numerical investigation of the laminar wakes generated by a curved plate conducted by Murali and Kumar [17] provided insight into the intricate relationships among the boundary layer, the separation bubble, and the wake zones. The arrangement of the wake flow in a turbulent boundary layer experiencing a pressure gradient downstream of a rib was studied experimentally by Güemes et al. [18].

Although much has been gained from these contributions, an extensive experimental analysis of the influence of the rectangle obstacle aspect ratio and Reynolds number on the friction coefficient of a flat plate in a turbulent boundary layer is still lacking. Moreover, almost all studies focus on circular and square obstacles, whereas only a few examine rectangular obstacles with a variety of aspect ratios. Thus, the current research aims to investigate the effect of rectangular obstacles with aspect ratios of 2, 4, 8, and 18 at four different Reynolds numbers on the friction coefficient of a flat plate using the floating-element technique.

## 2 | Experimental Method and Procedure

In this research, the floating-element technique was used to conduct experimental investigations of the effects of rectangular obstacles on the skin-friction coefficient of a flat plate in a turbulent boundary layer. As depicted in *Fig. 1*, a floating flat plate made of glass and placed in contact with the polished spherical bearing was used to provide minimal mechanical resistance to the air drag force created on the plate. In the floating technique, the plate moves freely along the flow's longitudinal direction due to aerodynamic drag. A bending load cell was used to measure the drag force acting on the flat plate. The drag force measurement was utilized to compute the skin-friction coefficient via *Eqs. (1) and (2)*.

$$\tau = \frac{F}{A}. \quad (1)$$

$$C_f = \frac{\tau_w}{\frac{1}{2}\rho U^2}, \quad (2)$$

where  $\tau_w$  is the wall shear stress.

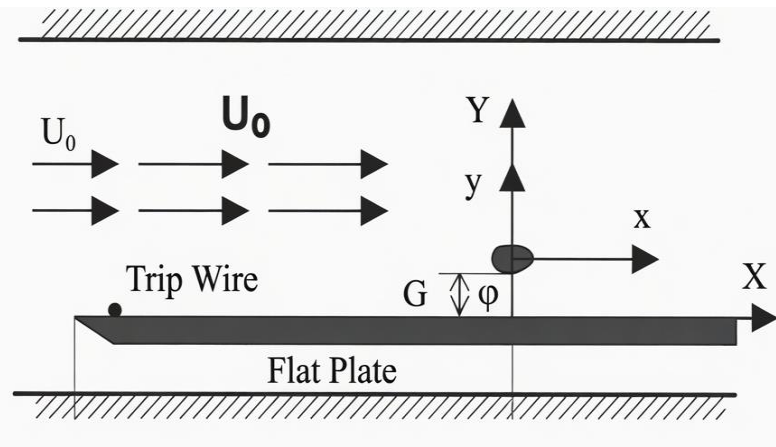


**Fig. 1. General schematic of the floating plate in the fluid flow path.**

The experiments were carried out in a suction-type wind tunnel with overall dimensions of 30 cm × 30 cm × 200 cm, as illustrated in *Fig. 3*. A glass plate of dimensions 30 cm x 200 cm was installed along the test section of the wind tunnel as the flat plate model. An axial fan placed in the downstream region of the wind tunnel created the airflow inside the wind tunnel. Given the cross-sectional area of the wind tunnel, the fan could generate a maximum air velocity of about 14 m/s. Air velocity and temperature were measured by a digital anemometer and a digital thermometer, respectively. To ensure the validity of the floating-element approach, the plate was made free to move along the spherical bearing.

In contrast, all possible spaces beneath the plate were sealed to prevent air leakage. Additionally, particular care was taken in designing the experiment to minimize interference between the flow direction and the leading and trailing edges of the plate, so that the flow would only go across the top surface of the plate. As a result of this design, the measured force reflected the wall shear stress arising from the development of the turbulent boundary layer.

Rectangular blocks having a thickness of  $t=0.8$  cm was used within the turbulent boundary layer, 144 cm away from the leading edge of the plate. They were placed within the boundary layer, maintaining a 2 mm gap from the plate surface. Four aspect ratio ( $c/t$ ) including 2, 4, 8, and 18 were selected for experimentation purposes.

In order to reduce the occurrence of disturbance and development of vortices as a consequence of the fan operation, the wind tunnel was operated in the suction mode in order to generate a more uniform turbulent flow over the surface of the plate. Additionally, diffusers were installed at both the inlet and outlet sections of the wind tunnel to prevent flow separation and vortices.

As an initial step towards verifying the experimental results, the skin friction coefficient was calculated for the smooth flat plate (i.e., no obstacle present) at Reynolds numbers corresponding to free-stream velocity of 10, 11, 12, and 14 m/s. In order to calculate the empirical relation between the turbulent flat plate, use:

$$C_{f_p} = 0.074(Re)^{-\frac{1}{5}}. \quad (3)$$

The comparison was intended to verify the accuracy of the experiment and its setup. Then, the identical measurements were repeated, this time with the rectangular obstacles, to investigate the impact of the aspect ratio and Reynolds number on the surface friction coefficient and the properties of the turbulent boundary layer.



**Fig. 2. Bending load cell for measuring drag force.**



**Fig. 3. Scheme of a wind tunnel with the axial fan at the outlet side.**

### 3 | Results and Discussion

To verify the test system and measurement conditions, the skin-friction coefficient for a smooth flat plate with no surface obstacles was determined experimentally at the selected Reynolds numbers. The values thus found were compared to the analytical relation for the skin-friction coefficient obtained through Eq. (3). This comparison is presented in Fig. 4. There is little deviation between the experimental values and the analytical relation, which is considered normal. Additionally, the skin-friction coefficient decreases with increasing Reynolds number.

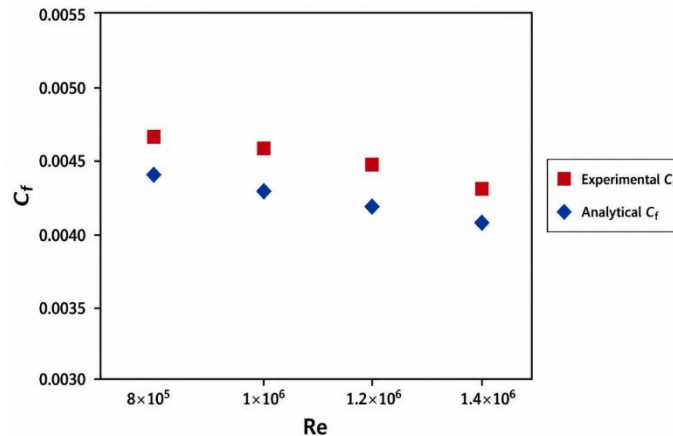


Fig. 4. Experimental and analytical skin-friction coefficients as a function of Reynolds number.

Once the experiments were validated for a smooth flat plate, the influence of rectangular obstacles with varying aspect ratios on the skin-friction coefficient was examined at different Reynolds numbers. Furthermore, the influence of increasing Reynolds number on drag reduction in the presence of obstacles was also studied. As shown in Fig. 5, the skin-friction coefficient ( $C_f$ ) varies as a function of Reynolds numbers for different obstacle aspect ratios.

Generally, the existence of obstacles within the turbulent boundary layer at a clearance distance of 2 mm from the surface of the plate caused a significant reduction in the skin-friction coefficient. As illustrated in Fig. 5, the lowest skin-friction coefficient occurs in the case of an obstacle with an aspect ratio of  $c/t=2$ . Therefore, it can be seen that smaller aspect-ratio obstacles cause a larger decrease in wall shear stress, resulting in lower friction drag on the flat plate. It is further noted that, in all cases with obstacles, the skin-friction coefficient decreases steadily as the Reynolds number increases.

Fig. 6 shows the reduction in the skin-friction coefficient of the considered obstacles relative to the smooth flat plate case at equal Reynolds numbers. The maximum reduction in the value of the friction factor is seen in the case of an aspect-ratio obstacle with  $c/t=2$ , highlighting the importance of aspect ratio of the obstacles in achieving drag reduction in turbulent flow.

In addition, the increasing values of Reynolds number contribute to drag reduction, as the highest reduction percentage is seen at the highest value of Reynolds number in the current study. Hence, it seems that vortex-turbulent boundary layer interaction plays a major role in determining the near-wall flow field.

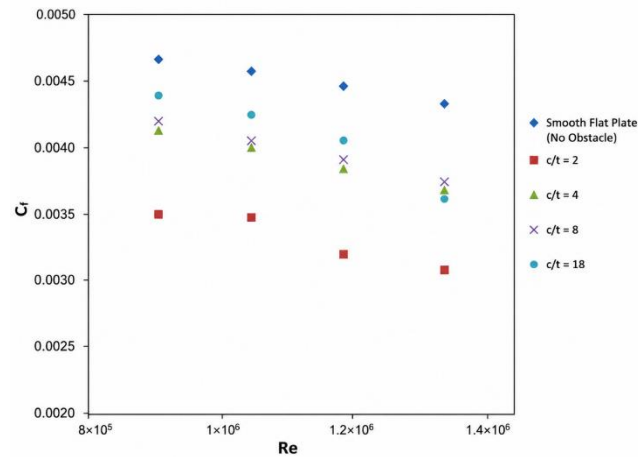


Fig. 5. Comparison of the skin-friction coefficient of the flat plate with obstacles of different aspect ratios vs. Reynolds number.

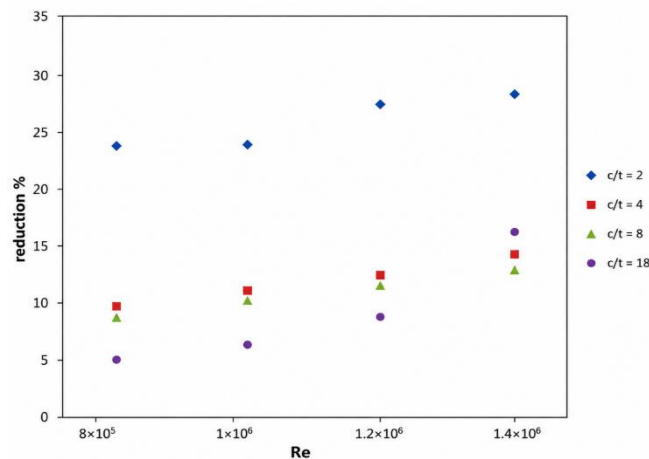


Fig. 6. Reduction percentage in skin-friction coefficient for different obstacle geometries in relation to the smooth flat plate at different Reynolds numbers.

## 4 | Conclusion

In this study, the influence of obstacles with different aspect ratios on the skin-friction coefficient of a flat plate in a turbulent boundary layer has been experimentally investigated using the floating-element technique in a suction-type wind tunnel. First, the accuracy of the experimental measurement system has been ensured by checking its outputs against theoretical skin-friction coefficient values calculated using available analytical correlations for turbulent flow past a smooth flat plate.

Experimental data show that introducing rectangular obstacles into the turbulent boundary layer reduces the skin-friction coefficient considerably. Among all tested obstacles, those with the minimum aspect ratio ( $c/t=2$ ) cause the greatest drag reduction on the flat plate. Moreover, a higher Reynolds number further decreases the skin-friction coefficient across all investigated obstacle aspect ratios.

Finally, it may be concluded that the interaction between the flow structures induced by the obstacles and the turbulent boundary layer affects flow behavior in the near-wall region, thereby decreasing wall shear stress on the plate. Based on the above results, one can conclude that the obstacle aspect ratio and Reynolds number are two significant factors contributing to drag reduction in turbulent flow past flat plates. On the whole, the

study demonstrates that well-designed rectangular protrusions located near the wall can reduce friction drag in the turbulent boundary layer. The results obtained can prove valuable for applications in the drag-reduction engineering field.

## Conflict of Interest

The authors report no conflicts of interest related to this work.

## Data Availability

All relevant data are presented in this manuscript.

## Funding

No financial support was received for the conduct of this study.

## References

- [1] Parker, R., & Welsh, M. C. (1983). Effects of sound on flow separation from blunt flat plates. *International journal of heat and fluid flow*, 4(2), 113–127. [https://doi.org/10.1016/0142-727X\(83\)90014-0](https://doi.org/10.1016/0142-727X(83)90014-0)
- [2] Stokes, A. N., & Welsh, M. C. (1986). Flow-resonant sound interaction in a duct containing a plate, II: Square leading edge. *Journal of sound and vibration*, 104(1), 55–73. [https://doi.org/10.1016/S0022-460X\(86\)80131-6](https://doi.org/10.1016/S0022-460X(86)80131-6)
- [3] Nakamura, Y., & Nakashima, M. (1986). Vortex excitation of prisms with elongated rectangular, H and [vdash ] cross-sections. *Journal of fluid mechanics*, 163, 149–169. <https://doi.org/10.1017/S0022112086002252>
- [4] Naudascher, E., & Wang, Y. (1993). Flow-induced vibrations of prismatic bodies and grids of prisms. *Journal of fluids and structures*, 7(4), 341–373. <https://doi.org/10.1006/jfls.1993.1021>
- [5] Park, T. S. (2013). Effects of an inserted square cylinder on wall heat transfer in laminar channel flows. *Journal of mechanical science and technology*, 27(5), 1501–1508. <https://doi.org/10.1007/s12206-013-0330-5>
- [6] Marumo, E., Suzuki, K., & Sato, T. (1985). Turbulent heat transfer in a flat plate boundary layer disturbed by a cylinder. *International journal of heat and fluid flow*, 6(4), 241–248. [https://doi.org/10.1016/0142-727X\(85\)90056-6](https://doi.org/10.1016/0142-727X(85)90056-6)
- [7] Suzuki, H., Suzuki, K., Kikkawa, Y., & Kigawa, H. (1990). Heat transfer and skin friction of a flat plate turbulent boundary layer disturbed by a cylinder. *Heat transfer-Japanese research;(United States)*, 20(2), 97–112.
- [8] de Souza, F., Delville, J., Lewalle, J., & Bonnet, J. P. (1999). Large scale coherent structures in a turbulent boundary layer interacting with a cylinder wake. *Experimental thermal and fluid science*, 19(4), 204–213. [https://doi.org/10.1016/S0894-1777\(99\)00022-9](https://doi.org/10.1016/S0894-1777(99)00022-9)
- [9] Kahrom, M., Haghparast, P., & Javadi, S. M. (2010). Optimization of heat transfer enhancement of a flat plate based on pareto genetic algorithm. *International journal of engineering*, 23, 177–189. [https://www.ije.ir/article\\_71853\\_a7e862a941c24a7b2198b708a9f3f426.pdf](https://www.ije.ir/article_71853_a7e862a941c24a7b2198b708a9f3f426.pdf)
- El Hassan, M., Bourgeois, J., & Martinuzzi, R. (2015). Boundary layer effect on the vortex shedding of wall-mounted rectangular cylinder. *Experiments in fluids*, 56(2), 33. <https://doi.org/10.1007/s00348-014-1882-6>
- [11] Isaev, S. A., Afanasiev, V. N., Egorov, K. S., & Kong, D. (2019). Experimental study of the influence of the shape of the gap between the rib and flat plate on the near-wall flow structure and heat transfer. *High temperature*, 57(3), 379–387. <https://doi.org/10.1134/S0018151X19030064>
- [12] Domel, A. G., Saadat, M., Weaver, J. C., Haj-Hariri, H., Bertoldi, K., & Lauder, G. V. (2018). Shark skin-inspired designs that improve aerodynamic performance. *Journal of the royal society interface*, 15(139), 20170828. <https://doi.org/10.1098/rsif.2017.0828>
- [13] Yang, S., Li, S., Tian, H., Wang, Q., & Jiang, N. (2015). Coherent spanwise structures in turbulent boundary layer over drag-reducing riblets. *Transactions of Tianjin University*, 21(4), 317–323. <https://doi.org/10.1007/s12209-015-2526-5>

- [14] Andreolli, A., Singh, M. K., & Gatti, D. (2024). Skin friction reduction via suppression of large scales in turbulent Couette flows. *International journal of heat and fluid flow*, 108, 109444. <https://doi.org/10.1016/j.ijheatfluidflow.2024.109444>
- [15] Beguet, S., Perraud, J., Forte, M., & Brazier, J. P. (2017). Modeling of transverse gaps effects on boundary-layer transition. *Journal of aircraft*, 54(2), 794–801. <https://doi.org/10.2514/1.C033647>
- [16] Rahman, H., Abbasi, W. S., Shams-ul-Islam, Khan, R., & Khan, M. U. (2021). Flow features of three side-by-side rectangular cylinders under the effect of aspect ratios and Reynolds numbers. *International journal of modern physics c*, 32(03), 2150034. <https://doi.org/10.1142/S0129183121500340>
- [17] Murali, D., & Ajithkumar, R. (2024). On the laminar wake of curved plates. *Physics of fluids*, 36(4), 43616. <https://doi.org/10.1063/5.0196430>
- [18] Güemes, A., Sanmiguel Vila, C., Örlü, R., Vinuesa, R., Schlatter, P., Ianiro, A., & Discetti, S. (2019). Flow organization in the wake of a rib in a turbulent boundary layer with pressure gradient. *Experimental thermal and fluid science*, 108, 115–124. <https://doi.org/10.1016/j.expthermflusci.2019.05.022>